ACS OMEGA

http://pubs.acs.org/journal/acsodf

Article

Reaction Behaviors and Crystal Transformation of Industrial Vanadium−Phosphorus−Oxygen (VPO) Catalysts for *n*-Butane Oxidation

Xia Zhang, Haibo Wang, Lianke Gou, Lanpeng Li, Aijun Duan,* and Zhengkai Cao*

Cite This: *ACS Omega* 2021, 6, 23558−23563

Read Online

ACCESS | Metrics & More | Article Recommendations | Supporting Information

ABSTRACT: A long-time evaluation of *n*-butane oxidation over an industrial vanadium−phosphorus−oxygen (VPO) catalyst was implemented. The catalytic performances for *n*-butane oxidation during this period were obtained. It was shown that the conversion of *n*-butane increased with the evaluation time, but the selectivity of the maleic anhydride (MA) product decreased gradually. To investigate the crystal transformation of the VPO catalyst, the properties of fresh and evaluated VPO catalysts were measured by a series of characterization methods, including X-ray diffraction (XRD), N_2 adsorption and desorption, NH_3-temperature programmed desorption (TPD), Raman spectroscopy, and X-ray photoelectron spectroscopy (XPS). The results showed that the acidities and valence of vanadium increased after evaluation due to the appearance of a β-$VOPO_4$ phase. The crystal transformation would increase the activity for *n*-butane oxidation. Meanwhile, during the evaluation period, the decrease in selectivity of the MA product should be related to the decreasing percentage of Lat-O species in the VPO catalyst.

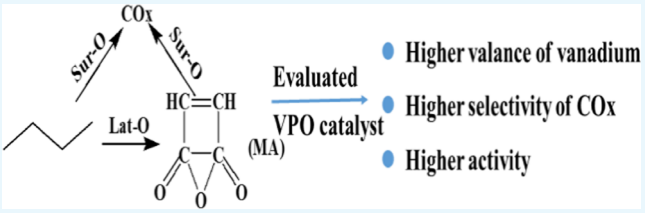

1. INTRODUCTION

Vanadyl pyrophosphate (VPO) catalysts have been proved to be effective for selectively oxidizing *n*-butane into maleic anhydride (MA).[1−3] The correlation of catalytic behaviors for *n*-butane oxidation with crystalline phases in VPO catalysts has been reviewed widely.[4−7] The crystalline phases can easily transform into other forms during calcination and activation. Therefore, it is really difficult to correlate the activity and selectivity with the crystalline phases.

Common VPO catalysts have $(VO)_2P_2O_7$ with a vanadium valence of 4+ and (α-, β-, γ-, δ-) $VOPO_4$ phases with a vanadium valence of 5+. The precursor $VOHPO_4{\cdot}0.5H_2O$ of the VPO catalyst will be transformed into V^{5+} and $(VO)_2P_2O_7$ phases in an oxidative atmosphere.[8] It has been reported that $(VO)_2P_2O_7$ will transform into the β-$VOPO_4$ phase in an oxygen atmosphere.[9] The β-$VOPO_4$ phase is treated as the most stable species among anhydrous orthophosphates.[8] The roles of V^{5+} and V^{4+} crystalline phases in the catalytic performance for *n*-butane oxidation were argued by many researchers.[10,11] Some believed that the $(VO)_2P_2O_7$ phase was considered as the active phase in the VPO catalyst for *n*-butane oxidation.[12] Others argued that the V^{5+}/V^{4+} dimeric species in the topmost oxidized layer of vanadyl pyrophosphate were the active sites.[13] Abon et al. reported that thestrong interaction of the isolated V^{5+} phase with the $(VO)_2P_2O_7$ phase would increase the selectivity of the MA product.[14] Mestl et al. found that a higher proportion of vanadyl pyrophosphate would lead to a more active catalytic performance. The surface amorphous V^{5+} species of the α-$VOPO_4$ phase could improve the activity for *n*-butane oxidation.[15] Above all, the crystalline phases of the VPO catalyst play an important role in the catalytic performance for *n*-butane oxidation.

Meanwhile, the stability of the VPO catalyst was significant for its industrial application. Patience et al. believed that carbon deposition was the primary cause of poor catalytic performance of the evaluated catalyst.[16] Li et al. studied the stability and reusability of a VPO catalyst. The authors assigned the deactivation to the carbon deposition on the active phase. They refreshed the used catalyst by calcination in an air atmosphere at 400 °C. However, the catalytic performance of the refreshed VPO catalyst was also decreased.[17]

In our work, a long-time evaluation of *n*-butane oxidation over an industrial VPO catalyst was implemented, and the changes of crystalline phases, pore parameters, and acidities between the fresh VPO catalyst and evaluated catalyst were compared carefully. The principle behind the change in conversion of *n*-butane and selectivity of the MA product with evaluation time was disclosed.

Received: July 10, 2021
Accepted: August 20, 2021
Published: September 1, 2021

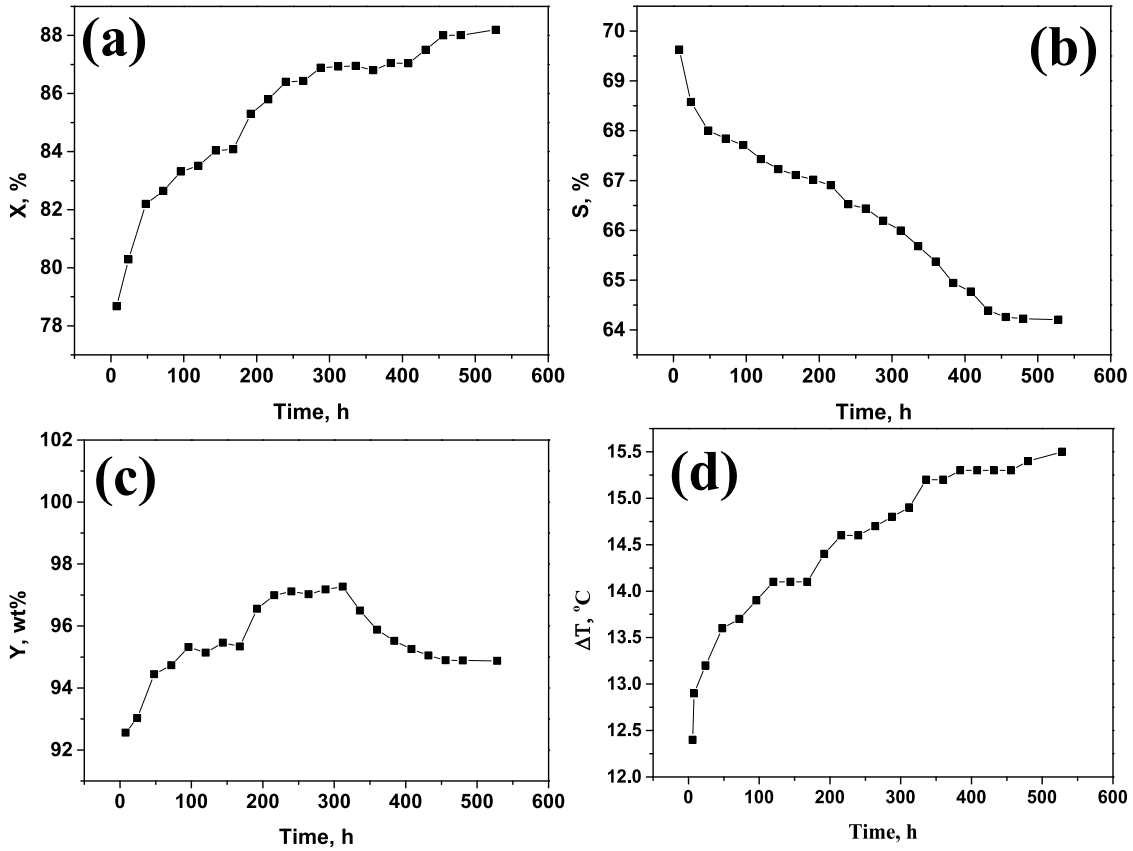

Figure 1. (a) Conversion of *n*-butane (X); (b) selectivity of MA (S); (c) mass yield of MA; and (d) temperature rise (ΔT).

2. EXPERIMENTAL SECTION

2.1. Catalyst. The industrial VPO catalyst was synthesized by Dalian Research Institute of Petroleum and Petrochemicals, SINOPEC. The preparation method was as follows: Isobutanol was selected as a reducing agent. V_2O_5 was applied as V sources, and phosphoric acid was chosen as P sources. Different raw materials for synthesis were mixed and reacted at 90 °C. The precursor was obtained and then dried in an air atmosphere. Thereafter, the obtained powder was mixed with a certain amount of graphite, and then the mixture was pressed into a tablet. Finally, the precursor was activated in a N_2/air (1:1) atmosphere at 390 °C with a temperature rising rate of 5 °C/h for 10 h.

2.2. Characterization Methods. The characterization methods for all of the VPO catalysts included N_2 adsorption−desorption, NH_3-TPD, X-ray diffraction (XRD), Raman spectroscopy, ammonia temperature-programmed desorption (NH_3-TPD), and X-ray photoelectron spectroscopy (XPS). The details of the above characterization methods are provided in the Supporting Information.

2.3. Evaluation Methods. Typically, 4.0 g of the VPO catalysts was used for the oxidation of *n*-butane to maleic anhydride. VPO catalysts with a mesh number of 10−20 were mixed with the same size silica sand (volume ratio 1:1). The mixture was loaded in the middle of a stainless-steel fixed-bed reactor. The reactor diameter was 14 mm. The length of the catalyst bed was about 7.0 cm. The position of a thermocouple would be adjusted at the hot point of the catalyst bed at different reaction conditions. The gas feed consisted of *n*-butane and air, and the volume percentage of *n*-butane was 1.392%. The oxidation of *n*-butane over all of the VPO catalysts was evaluated under the conditions of P = 0.03 MPa, T = 400 °C, and gas hourly space velocity (GHSV) = 2000 h^{-1}. The outlet gas stream from oxidation of *n*-butane for all of the catalysts was analyzed by gas chromatography (Agilent).

2.4. Calculation Methods. The *n*-butane conversion (X), selectivity of the MA product (S), and yields of the MA product (Y) were calculated by the following equations

$$X = \frac{yn_{in} - yn_{out}}{yn_{in}} \quad (1)$$

$$S = 1 - \frac{(y_{CO} + y_{CO_2})}{4(yn_{in} - yn_{out})} \quad (2)$$

$$Y = X \times S \quad (\text{mol}\%) \quad (3)$$

In the above equations, y represents the volume or molar percentage; yn_{in} and yn_{out} represent the volume percentages of *n*-butane in the feed and product, respectively; and y_{CO} and y_{CO2} represent the volume percentages of CO and CO_2 (CO_x) in the gas product, respectively.

3. RESULTS AND DISCUSSION

3.1. Long-Time Evaluation for the VPO Catalyst. The *n*-butane oxidation performance of the industrial VPO catalysts was evaluated for 528 h. The conversion of *n*-butane (X), selectivity of MA (S), mass yield of MA, and temperature rise (ΔT) were obtained and are shown in Figure 1. It presented that the conversion of *n*-butane increased with the evaluation time. After evaluation for 528 h, the X values increased from 78.67 to 88.20%. However, the selectivity of the MA product decreased with the evaluation time. The S values decreased

https://doi.org/10.1021/acsomega.1c03652
ACS Omega 2021, 6, 23558−23563

from 68.44 to 64.33%. As reported in the literature, the selectivity of the MA product for a typical VPO catalyst was about 56%, which was lower than our prepared catalyst. Moreover, the mass yield of the MA product increased with the evaluation time before 312 h. Thereafter, the mass yield of the MA product decreased sharply from 97.37 to 95.87%. The temperature rise also increased with the evaluation time, which indicated that the activity increased with the evaluation time. In addition, the selectivities of CO and CO_2 products during the long-time evaluation period are also shown in Figure S1. It showed that the selectivity of CO_2 increased from 11.1 to 14.1%, and the selectivity of CO increased from 18.1 to 21.1% gradually. Accordingly, it was significant to clarify the mechanism of the dramatic change in the *n*-butane oxidation performance of the VPO catalyst during such a short time.

3.2. Properties of Fresh and Evaluated Catalysts. To investigate the change of pore properties for fresh and evaluated VPO catalysts, N_2 adsorption and desorption measurements were applied. The result is shown in Figure 2,

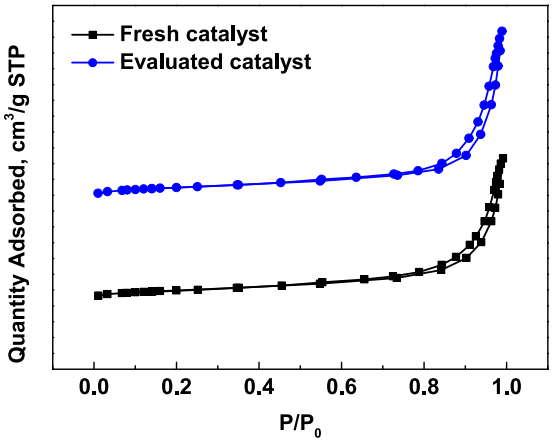

Figure 2. N_2 adsorption−desorption isotherm of fresh and evaluated catalysts.

and the pore properties of fresh and evaluated VPO catalysts are given in Table 1. From Figure 2, fresh and evaluated

Table 1. Properties of Fresh and Evaluated Catalysts

catalyst	fresh catalyst	evaluated catalyst
surface area, m^2/g	27.72	27.39
volume, cm^3/g	0.14	0.16
pore diameter, nm	20.35	23.96
P contents, wt %	18.97	18.48

catalysts showed type V curves with H3 hysteresis loops. As shown in Table 1, the surface area of the evaluated catalyst was lower than that of the fresh catalyst. The pore volume and pore diameter of the evaluated catalyst were higher than those of the fresh catalyst. In general, the pore properties of fresh and evaluated catalysts had a small change. Moreover, the contents of phosphorus in the fresh and evaluated catalysts were 18.97 and 18.48 wt %, respectively. This could indicate that a phosphorus loss would occur during the long-time evaluation. The phosphorus loss would influence the crystal composition and catalytic behaviors. It has been reported that the phosphorus loss would decrease the selectivity of the MA product. The catalyst must compensate for the loss of phosphorus to maintain stable operation at a certain time.[3,18−20]

NH_3-TPD spectra were used to determine the acidities of fresh and evaluated catalysts. The NH_3-TPD patterns and acidities of the two catalysts are shown in Figure 3 and Table 2,

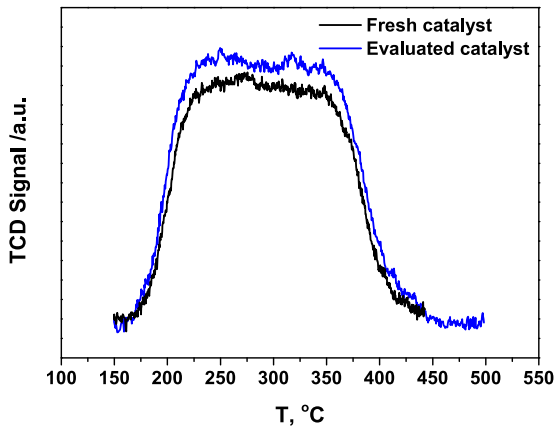

Figure 3. NH_3-TPD patterns of fresh and evaluated catalysts.

Table 2. Acidities of Fresh and Evaluated Catalysts

catalyst	150−250 °C, mL/g	250−400 °C, mL/g	400−450 °C, mL/g	total amount, mL/g
fresh catalyst	1.378	2.124	0.794	4.306
evaluated catalyst	1.776	2.212	0.883	4.871

respectively. The strengths of acidities were assigned as weak (150−250 °C), medium (250−400 °C), and strong (400−450 °C) on the basis of NH_3 desorption temperatures. It was shown that the total amount of acidity of the evaluated catalyst was higher than that of the fresh catalyst. Noticeably, V^{5+} species could accept an electron and transform into V^{4+}. V^{5+} species could be considered as Lewis acid sites. Meanwhile, it has been reported that the amount of Lewis sites for VPO catalysts is more higher than that of Bronsted sites.[21] Therefore, it could be deduced that the percentage of V^{5+} species on the surface of the catalyst would be increased due to the increment of total acidity.

The XRD measurement was implemented to investigate the crystal transformation of fresh and evaluated catalysts, and the corresponding patterns are shown in Figure 4. For the fresh catalyst, the peaks appearing at 18.5, 21.7, 23.0, 28.5, 29.9, 33.7, 36.4, and 38.1° should be ascribed to the $(VO)_2P_2O_7$ phase with the (020), (113), (200), (024), (032), (016), (230), and (232) crystal faces, respectively.[22,23] For the evaluated catalyst, the peak at 21.7° assigned to the $(VO)_2P_2O_7$ phase could not be observed. However, the new peak at 29.3° assigned to the β-$VOPO_4$ phase from the (020) direction could be observed. The vanadium valence of the $(VO)_2P_2O_7$ phase was 4+, and the vanadium valence of the β-$VOPO_4$ phase was 5+.[8] Accordingly, the vanadium valence of the VPO catalyst would be increased after evaluation due to the appearance of the β-$VOPO_4$ crystal phase.

The more sensitive Raman measurement was applied to study the crystal changes of fresh and evaluated catalysts. The Raman spectra are shown in Figure 5. It exhibited that the crystal phases of the VPO catalyst changed a lot after

https://doi.org/10.1021/acsomega.1c03652
ACS Omega 2021, 6, 23558−23563

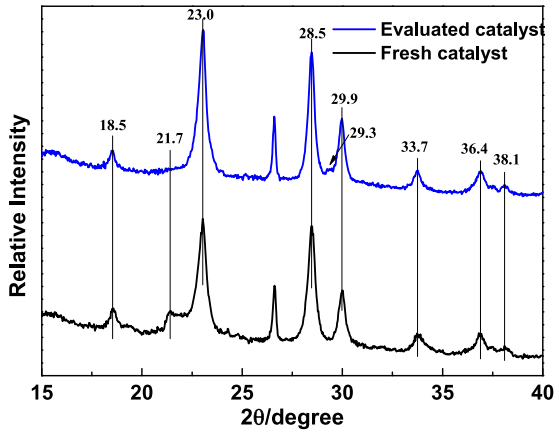

Figure 4. XRD patterns of fresh and evaluated catalysts.

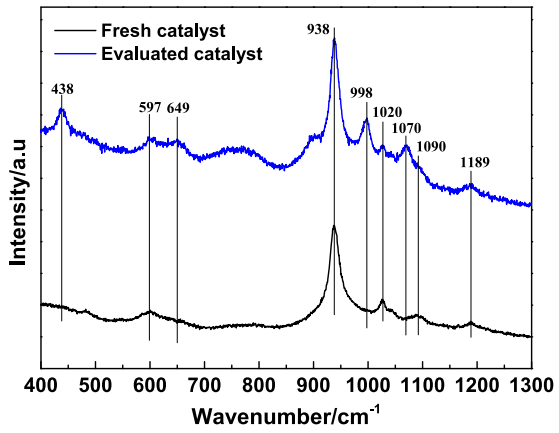

Figure 5. Raman spectra of fresh and evaluated catalysts.

evaluation. For the fresh catalyst, the peaks at about 597, 649, 938, 1020, 1090, and 1186 cm^{-1} were assigned to the $(VO)_2P_2O_7$ crystal phase. For the evaluated catalyst, some new peaks at about 438, 998, and 1070 cm^{-1} were ascribed to the β-$VOPO_4$ phase.[6,23,24] Therefore, the appearance of the β-$VOPO_4$ phase would occur after the long-time evaluation. This could lead to the increment of vanadium valence for the VPO catalyst, which was in accordance with the XRD measurement.

The XPS measurement was used to study the surface V and O species of fresh and evaluated catalysts.[12,25] The XPS spectra of fresh and evaluated catalysts in the V $2p_{3/2}$ and O 1s regions are shown in Figures 6 and 7, respectively. The obtained percentages of V^{4+} and V^{5+}, average vanadium valence, and Lat-O/Sur-O ratio are given in Table 3. The binding energies from 528 to 536 eV were assigned to O 1s species of the VPO catalyst.[26,27] The existent states of oxygen species over the VPO catalyst included surface hydroxide ions and carbonates (Sur-O) and lattice oxygen ions (Lat-O).[28,29] The binding energy of Sur-O species was 533.1 eV, and the binding energy of Lat-O species was nearly 532.1 and 531.1 eV.[26,30] From Table 3, compared with the fresh VPO catalyst, the Lat-O/Sur-O ratio decreased from 1.39 to 1.30 after the long-time evaluation.

In Figure 7, the binding energies from 512 to 520 eV were ascribed to V $2p_{3/2}$ species in the VPO catalyst. It has been reported that the binding energies of V^{4+} and V^{5+} species were 516.8 and 517.8 eV, respectively.[31,32] As shown in Table 3, the percentage of V^{5+} and average vanadium valence of the

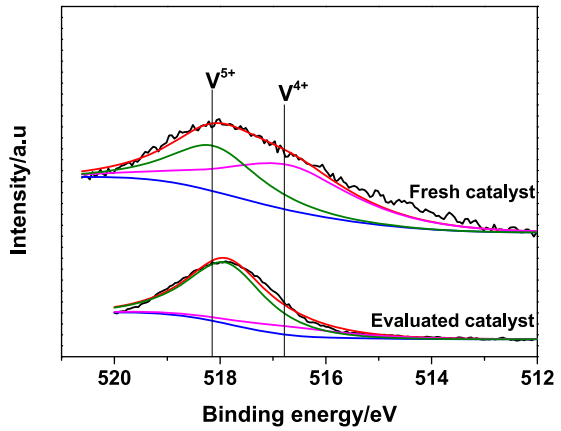

Figure 6. XPS spectra in the V $2p_{3/2}$ region for fresh and evaluated catalysts.

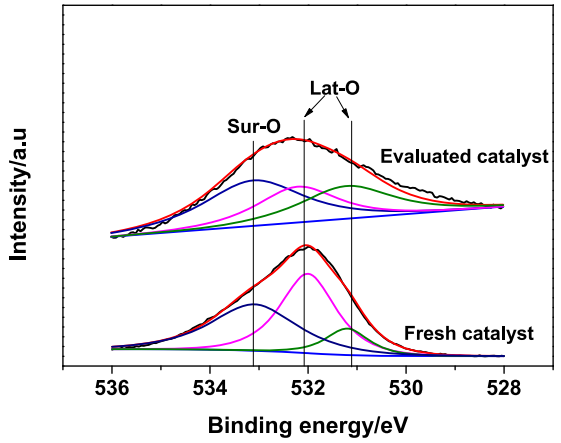

Figure 7. XPS spectra in the O 1s region for fresh and evaluated catalysts.

Table 3. XPS Data of Different Catalysts

catalysts	P (V^{4+})	P (V^{5+})	V_{av}[a]	Lat-O/Sur-O
fresh catalyst	0.59	0.41	4.41	1.39
evaluated catalyst	0.13	0.87	4.87	1.30

[a] $V_{av} = 4 \times P\ (V^{4+}) + 5 \times P\ (V^{5+})$.

evaluated VPO catalyst were higher than those of the fresh VPO catalyst. The XPS results were consistent with the NH_3-TPD, XRD, and Raman measurements. Ait-Lachgar et al. proposed that the Sur-O species was associated with the appearance of V^{5+} ions.[14] In our experiment, the increased vanadium valence and percentage of Sur-O species for the VPO catalyst after evaluation confirmed the above proposition.

3.3. Mechanism of Crystal Phase Transformation. The pore property, acidity, crystal phases, and nature of oxygen species of VPO catalysts would play an important role in the catalytic performance for *n*-butane oxidation. The N_2 adsorption and desorption results showed that the pore diameter, pore volume, and surface area changed little after the long-time evaluation. However, the amount of acidity for the VPO catalyst was increased after evaluation. It has been reported that the acid sites could particularly activate *n*-butane molecules.[33] If the acid sites were poisoned by NH_3 or K, the reaction of *n*-butane to MA would be strongly prohibited.[34,35]

https://doi.org/10.1021/acsomega.1c03652
ACS Omega 2021, 6, 23558−23563

Therefore, the increase in conversion of *n*-butane should be correlated with the increase in acidity. Moreover, the transformation of the crystal phase for the VPO catalyst would also occur during the evaluation period. The XRD, Raman, and XPS measurements confirmed that the vanadium valence was increased due to the existence of the β-$VOPO_4$ phase after the long-time evaluation. Some researchers compared a $(VO)_2P_2O_7$ catalyst without V^{5+} species and a conventional VPO catalyst with V^{5+} species. It was revealed that the presence of residual V^{5+} entities on the V^{4+} matrix could favor the conversion of *n*-butane to MA.[36] Some researchers also disclosed that the isolated V^{5+} sites in strong interaction with $(VO)_2P_2O_7$ were important in the selective oxidation of *n*-butane to MA, and the best V^{5+}/V^{4+} ratio should be 0.25. Therefore, the fact that the activity of *n*-butane oxidation showed an increasing trend in our experiment should also be associated with the increasing percentage of V^{5+} in the VPO catalyst. In conclusion, the increase in conversion of *n*-butane and selectivities of CO and CO_2 during the long-time evaluation should be due to the increase in vanadium valence and acidity of the VPO catalyst.

The reaction path of *n*-butane oxidation is shown in Scheme 1. The Lat-O species could facilitate the formation of the MA

Scheme 1. Reaction Path of *n*-Butane Oxidation

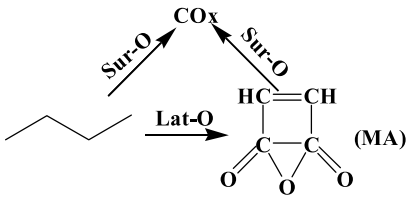

product, while the Sur-O species could lead to the deep oxidation into CO_x.[37] Hence, the Lat-O/Sur-O ratio might be well related to the selectivity of the MA product in the oxidation of *n*-butane. The evaluated VPO catalyst showed a lower Lat-O/Sur-O ratio than the fresh catalyst. The selectivity of the MA product presented a decreasing trend during the long-time evaluation, which should be caused by the loss of Lat-O species.

4. CONCLUSIONS

An industrial VPO catalyst was evaluated for a long time. The results showed that the conversion of *n*-butane and reaction activities increased with running time. However, the selectivity of the MA product decreased with the running time. At a certain time, the yield of the MA product decreased sharply.

The properties of fresh and evaluated VPO catalysts were compared systematically. The characterization results revealed that the acidities and valence state of vanadium of the evaluated VPO catalyst were higher than those of the fresh catalyst due to the appearance of the β-$VOPO_4$ phase. The crystal transformation of the VPO catalyst would promote the oxidation of *n*-butane.

Finally, the influences of crystal phase transformation on the activity for *n*-butane oxidation and selectivity of the MA product were revealed. The increasing activities should be due to the increasing percentage of V^{5+} in the VPO catalyst. The decreasing selectivity of the MA product should be due to the decreasing percentage of Lat-O species.

■ ASSOCIATED CONTENT

Supporting Information

The Supporting Information is available free of charge at https://pubs.acs.org/doi/10.1021/acsomega.1c03652.

Detailed characterization methods for fresh and evaluated catalysts and selectivities of CO and CO_2 products during the long-time evaluation period (Figure S1) (PDF)

■ AUTHOR INFORMATION

Corresponding Authors

Aijun Duan − *State Key Laboratory of Heavy Oil Processing, China University of Petroleum, Beijing 102249, China;* orcid.org/0000-0001-5964-7544; Email: duanaijun@cup.edu.cn

Zhengkai Cao − *Dalian Research Institute of Petroleum and Petrochemicals, SINOPEC, Dalian 116045 Liaoning, China; State Key Laboratory of Heavy Oil Processing, China University of Petroleum, Beijing 102249, China;* orcid.org/0000-0003-2058-9783; Email: xiaocao19910926@163.com

Authors

Xia Zhang − *Dalian Research Institute of Petroleum and Petrochemicals, SINOPEC, Dalian 116045 Liaoning, China*

Haibo Wang − *Dalian Research Institute of Petroleum and Petrochemicals, SINOPEC, Dalian 116045 Liaoning, China*

Lianke Gou − *Dalian Research Institute of Petroleum and Petrochemicals, SINOPEC, Dalian 116045 Liaoning, China*

Lanpeng Li − *Dalian Research Institute of Petroleum and Petrochemicals, SINOPEC, Dalian 116045 Liaoning, China*

Complete contact information is available at: https://pubs.acs.org/10.1021/acsomega.1c03652

Notes

The authors declare no competing financial interest.

■ ACKNOWLEDGMENTS

The authors thank the National Natural Science Foundation of China (Project Nos. 21878330, 21676298, and 21808079) for supporting their research.

■ REFERENCES

(1) Paunović, V.; Zichittella, G.; Moser, M.; Amrute, A. P.; Perez-Ramirez, J. Catalyst design for natural-gas upgrading through oxybromination chemistry. *Nat. Chem.* **2016**, *8*, 803−809.

(2) Wang, P.; Fu, G.; Wan, H. How High valence transition metal spreads its activity over nonmetal oxoes: A proof-of-concept study. *ACS Catal.* **2017**, *7*, 5544−5548.

(3) Müller, M.; Kutscherauer, M.; Böcklein, S.; Wehinger, G. D.; Turek, T.; Mestl, G. Modeling the selective oxidation of n-butane to maleic anhydride: From active site to industrial reactor. *Catal. Today* **2021**, DOI: 10.1016/j.cattod.2021.04.009.

(4) Centi, G.; Trifiro, F.; Ebner, J. R.; Franchetti, V. M. Mechanistic aspects of maleic anhydride synthesis from C4 hydrocarbons over phosphorus vanadium oxide. *Chem. Rev.* **1988**, *88*, 55−80.

(5) Centi, G. Vanadyl Pyrophosphate - A Critical Overview. *Catal. Today* **1993**, *16*, 5.

(6) Cavani, F.; Santi, D. D.; Luciani, S.; Löfberg, A.; Bordes-Richard, E.; Cortelli, C.; Leanza, R. Transient reactivity of vanadyl pyrophosphate, the catalyst for n-butane oxidation to maleic anhydride, in response to in-situ treatments. *Appl. Catal., A.* **2010**, *376*, 66−75.

(7) Santra, C.; Shah, S.; Mondal, A.; Pandey, J. K.; Panda, A. B.; Maity, S.; Chowdhury, B. Synthesis, characterization of VPO catalyst dispersed on mesoporous silica surface and catalytic activity for cyclohexane oxidation reaction. *Microporous Mesoporous Mater.* **2016**, *223*, 121−128.
(8) Xue, Z. Y.; Schrader, G. L. In situ laser Raman spectroscopy studies of VPO catalyst transformations. *J. Phys. Chem. B* **1999**, *103*, 9459−9467.
(9) Bordes, E.; Courtine, P. J. Some selectivity criteria in mild oxidation catalysis: VPO phases in butene oxidation to maleic anhydride. *J. Catal.* **1979**, *57*, 236−252.
(10) Dinh, M. T. N.; Nguyen, T. L.; Phan, M. D.; Dinh, L. N.; Bordes-Richard, E.; et al. Control of the crystal morphology of $VOHPO_4 0.5H_2O$ precursors prepared via light alcohols-assisted solvothermal synthesis and influence on the selective oxidation of n-butane. *J. Catal.* **2019**, *377*, 638−651.
(11) Cavani, F.; Ligi, S.; Monti, T.; Pierelli, F.; Mazzoni, G.; et al. Relationship between structural/surface characteristics and reactivity in n-butane oxidation to maleic anhydride: the role of V^{3+} species. *Catal. Today* **2000**, *61*, 203−210.
(12) He, B.; Li, Z.; Zhang, H.; Dai, F.; Li, K.; Liu, R.; Zhang, S. Synthesis of vanadium phosphorus oxide catalysts assisted by deep-eutectic solvents for n-Butane selective oxidation. *Ind. Eng. Chem. Res.* **2019**, *58*, 2857−2867.
(13) Hodnett, B. K. Vanadium-phosphorus oxide catalysts for the selective oxidation of c4 hydrocarbons to maleic anhydride. *Catal. Rev.* **1985**, *27*, 373−424.
(14) AïT-Lachgar, K.; Tuel, A.; Brun, M.; Herrmann, J. M.; Krafft, J. M.; Martin, J. R.; Volta, J. C.; Abon, M. Selective oxidation of n-butane to maleic anhydride on vanadyl pyrophosphate. II. Characterization of the oxygen-treated catalyst by electrical conductivity, Raman, XPS and NMR spectroscopies. *J. Catal.* **1998**, *177*, 383−390.
(15) Böcklein, S.; Mestl, G.; Auras, S. V.; Wintterlin, J. On the correlation of structure and catalytic performance of VPO Catalysts. *Top. Catal.* **2017**, *60*, 1682−1697.
(16) Patience, G. S.; Bockrath, R. E.; Sullivan, J. D.; Horowitz, H. S. Pressure calcination of VPO catalyst. *Ind. Eng. Chem. Res.* **2007**, *46*, 4374−4381.
(17) Yang, D.; Sararuk, C.; Suzuki, K.; Li, Z.; Li, C. Effect of calcination temperature on the catalytic activity of VPO for aldol condensation of acetic acid and formalin. *Chem. Eng. J.* **2016**, *300*, 160−168.
(18) Lesser, D.; Mestl, G.; Turek, T. Transient behavior of vanadyl pyrophosphatecatalysts during the partial oxidation of n-butane in industrial-sized, fixed bed reactors. *Appl. Catal., A* **2016**, *510*, 1−10.
(19) Lesser, D.; Mestl, G.; Turek, T. Modeling the dynamic behavior of industrial fixed bed reactors for the manufacture of maleic anhydride. *Chem. Eng. Sci.* **2017**, *172*, 559−570.
(20) Mestl, G.; Lesser, D.; Turek, T. Optimum performance of vanadyl pyrophosphate Catalysts. *Top. Catal.* **2016**, *59*, 1533−1544.
(21) Abon, M.; Volta, J. C. Vanadium phosphorus oxides for n-butane oxidation to maleic anhydride. *Appl. Catal., A* **1997**, *157*, 173−193.
(22) Ben Abdelouahab, F.; Olier, R.; Guilhaume, N.; Lefebvre, F.; Volta, J. C. A Study by in situ Laser Raman Spectroscopy of VPO Catalysts for n-Butane Oxidation to Maleic Anhydride. *J. Catal.* **1992**, *134*, 151−167.
(23) Batis, N. H.; Batis, H.; Ghorbel, A.; Vedrine, J. C.; Volta, J. C. Synthesis and characterization of new VPO catalysts for partial n-Butane oxidation to maleic anhydride. *J. Catal.* **1991**, *128*, 248−263.
(24) Bordes, E.; Courtine, P. New phases in V-P-O catalysts and their role in oxidation of butane to maleic anhydride. *J. Chem. Soc., Chem. Commun.* **1985**, 294−296.
(25) Behera, G. C.; Parida, K. M.; Das, D. P. Facile fabrication of aluminum-promoted vanadium phosphate: A highly active heterogeneous catalyst for isopropylation of toluene to cymene. *J. Catal.* **2012**, *289*, 190−198.
(26) Luciani, S.; Cavani, F.; Santo, V. D.; Dimitratos, N.; Rossi, M.; Bianchi, C. L. The mechanism of surface doping in vanadyl pyrophosphate, catalyst for n-butane oxidation to maleic anhydride: The role of Au promoter. *Catal. Today* **2011**, *169*, 200−206.
(27) Ait-Lachgar, K.; Tuel, A.; Brun, M.; Herrmann, J. M.; Krafft, J. M.; Martin, J. R.; Volta, J. C.; Abon, M. Selective oxidation of nbutane to maleic anhydride on vanadyl pyrophosphate characterization of the oxygen-treated catalyst by electrical conductivity, Raman, XPS, and NMR spectroscopic techniques. *J. Catal.* **1998**, *177*, 224−230.
(28) Abon, M.; Bere, K. E.; Tuel, A.; Delichere, P. Evolution of a VPO Catalyst in n-Butane Oxidation Reaction During the Activation Time. *J. Catal.* **1995**, *156*, 28−36.
(29) Solsona, B.; Zazhigalov, V. A.; López Nieto, J. M.; Bacherikova, I. V.; Diyuk, E. A. Oxidative dehydrogenation of ethane on promoted VPO catalysts. *Appl. Catal., A.* **2003**, *249*, 81−92.
(30) Stoch, J.; Gablankowskakukucz, J. The effect of carbonate contaminations on the XPS-O-1s band-structure in metal-oxides. *Surf. Interface Anal.* **1991**, *17*, 165−167.
(31) Richter, F.; Papp, H.; Wolf, G. U.; Götze, T.; Kubias, B. Study of the surface composition of vanadyl pyrophosphate catalysts by XPS and ISS-Influence of Cs+ and water vapor on the surface P/V ratio of $(VO)_2P_2O_7$ catalysts. *Fresenius J. Anal. Chem.* **1999**, *365*, 150−153.
(32) Guan, J.; Wang, Z.; Xu, C.; Yang, Y.; Liu, B.; Yu, X.; Kan, Q. Partial Oxidation of Isobutane over Vanadium Phosphorus Oxides. *Catal. Lett.* **2009**, *128*, 356−362.
(33) Busca, G.; Centi, G.; Trifiro, F. N-butane selective oxidation on vanadium-based oxides: dependence on catalyst microstructure. *Appl. Catal.* **1986**, *25*, 265−272.
(34) Busca, G.; Centi, G.; Trifiro, F.; Lorenzelli, V. Surface acidity of vanadyl pyrophosphate, active phase in n-butane selective oxidation. *J. Phys. Chem. A* **1986**, *90*, 1337−1344.
(35) Puttock, S. J.; Rochester, C. H. Infrared study of water and pyridine adsorption on the surface of anhydrous vanadyl pyrophosphate. *J. Chem. Soc., Faraday Trans. 1* **1986**, *82*, 2773−2779.
(36) Zhang-Lin, Y.; Forissier, M.; Sneeden, R. P.; Vedrine, J. C.; Volta, J. C. On the mechanism of n-butane oxidation to maleic anhydride on VPO catalysts. I. A kinetics study on a VPO catalyst as compared to VPO reference phases. *J. Catal.* **1994**, *145*, 256−266.
(37) Arnold, E. W.; Sundaresan, S. Dynamics of packed-bed reactors loaded with oxide catalysts. *AIChE J.* **1989**, *35*, 746−754.

https://doi.org/10.1021/acsomega.1c03652
ACS Omega 2021, 6, 23558−23563